Progress In Electromagnetics Research C, Vol. 5, 149–168, 2008

WIRELESS BIO-RADAR SENSOR FOR HEARTBEAT AND RESPIRATION DETECTION

B.-J. Jang

Department of Electrical Engineering
Kookmin University
861-1 Jeongneung-dong, Seonbuk-Ku, Seoul, 136-702, Korea

S.-H. Wi and J.-G. Yook

Department of Electrical Engineering
Yonsei University
134 Shinchon-dong, Seodaemoon-Ku, Seoul, 120-749, Korea

M.-Q. Lee

Department of Electronic, Electrical and Computer Engineering
University of Seoul
90 Jeonnong-dong, Dongdaemun-Ku, Seoul, 130-743, Korea

K.-J. Lee

Department of Biomedical Engineering
Yonsei University
234 Maeji-ri, Heungup-myun, Wounju-si, Gangwon-do 220-710, Korea

Abstract—In this study, a wireless bio-radar sensor was designed to detect a human heartbeat and respiration signals without direct skin contact. In order to design a wireless bio-radar sensor quantitatively, the signal-to-noise ratio (SNR) in the baseband output of a sensor should be calculated. Therefore, we analyzed the SNR of the wireless bio-radar sensor, considering the signal power attenuation in a human body and all kinds of noise sources. Especially, we measured a residual phase noise of a typical free-running oscillator and used its value for the SNR analysis. Based on these analysis and the measurement results, a compact, low-cost 2.4 GHz direct conversion bio-radar sensor was designed and implemented in a printed circuit board. The demonstrated sensor consists of two printed antennas, a

voltage-controlled oscillator, an I/Q demodulator, and analog circuits. The heartbeat and respiration signals acquired from the I/Q channel of the sensor are applied to the digital signal processing circuit using MATLAB. ECG (electrocardiogram), and reference respiration signals are measured simultaneously to evaluate the performance of the sensor. With an output power of 0 dBm and a free running oscillator without a phase locked loop circuits, a detection range of 50 cm was measured. Measurement results show that the heart rate and respiration accuracy was very high. Therefore, we verified that a wireless bio-radar sensor could detect heartbeat and respiration well without contact and our SNR analysis could be an effective tool to design a wireless bio-radar sensor.

1. INTRODUCTION

Recently, a wireless bio-radar sensor, fabricated using Doppler theory, has drawn a great deal of attention as a non-contact monitoring system for human healthcare and vital-sign monitoring, such as in cardiopulmonary monitoring for sleep apnea syndrome detection [1]. To measure heartbeat and respiration signals, direct contact measurement using electrodes attached to the skin is generally practiced. The direct contact measurement has difficulties in measuring bio-signals continuously and in being applied to an infant or a patient with severe burns. In addition, problems of infection and uncomfortableness are inherent in the direct contact measurement. Therefore, a wireless bio-radar sensor needs to be designed in order to measure heartbeat and respiration signals without direct skin contact.

Typically, a wireless sensor transmits a continuous-wave (CW) signal and demodulates the signal reflected off of a human chest-wall. Consistent with Doppler theory, a human chest-wall has a time-varying position with net zero velocity and will reflect a signal with its phase-modulated in proportion to the position of the chest-wall. By demodulating this phase-modulated signal, heart and respiration rates could be obtained. Based on this principle, a wireless bio-radar sensor was first applied to the measurement of respiration rate and the detection of apnea in 1975 [2]. Because of the range correlation effect that reduces close-in phase noise, direct-conversion receiver chips with free-running oscillators were able to detect low-frequency heartbeat and respiration without using external crystal and phase-locked loop (PLL) circuits [3, 4]. Also, the null-point issue encountered in general wireless sensors was also avoided by using a quadrature receiver approach [5].

However, these previous studies mainly focused on receiver architectures and signal processing algorithms, making it difficult to extract the system design parameters directly. In order to simplify the wireless bio-radar sensor design, a signal-to-noise ratio (SNR) analysis is needed, which is commonly used in wireless communication and radar systems. A SNR analysis uses the simple path loss value and various noise effects at the baseband output as design variables. Exact SNR analysis is particularly important when measuring the motion due to heartbeat, since the information is encoded in phase modulations of 0.1 to 10 Hz, where the phase noise is near the peak. To date, there have been few studies about the SNR analysis of a wireless bio-radar sensor. In [6], the measured flicker noise was considered as a dominant noise sources without exact SNR analysis. Only in [7] was the exact SNR value including the phase noise of the reflected clutter signal analyzed. However, its results did not considered various phase noises due to antenna and mixer leakage signals as noise source.

In this paper, therefore, we show the SNR analysis including the path loss in a human body and all kinds of noise powers. Especially, we measured a baseband phase noise of a typical free-running oscillator and used this value for the SNR analysis. Based on these analysis and measurement results, we demonstrate a design example of wireless bio-radar sensor operating at the frequency of the 2.4 GHz Industrial, Scientific, and Medical (ISM) band. We have designed the whole system, from antenna to baseband, to make a compact, low-cost, portable bio-radar sensor.

2. OPERATING PRINCIPLE OF A WIRELESS BIO-RADAR SENSOR

Typical wireless bio-radar sensor architecture is shown in Fig. 1. A sensor is made up of two blocks: the wireless transceiver block, which is used to generate a CW signal and convert the reflected signal to a baseband signal, and the digital signal processing (DSP) block, which is used to determine heart and respiration rates.

In the wireless transceiver block, a single oscillator generates both the transmitted RF and local oscillator (LO) signals. When the CW signal is directed at a target, it is reflected and frequency-modulated by the target motion. If the target undergoes a periodic movement $x(t)$ with no net velocity, the Doppler shift of the reflected signal can be described as a phase modulation as shown in (1),

$$\theta(t) = \frac{2f}{c}(2\pi x(t)) = \frac{4\pi x(t)}{\lambda} \tag{1}$$

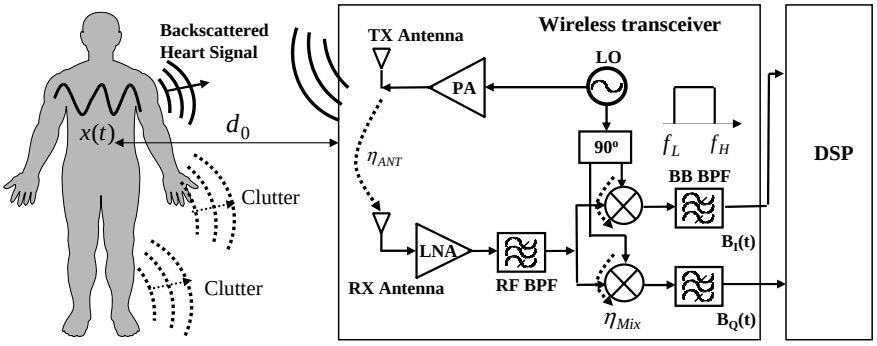

Figure 1. Heartbeat and respiration detection using a wireless bio-radar sensor.

where f is the transmitted frequency in Hz, c is the signal propagation velocity in m/s, and λ is the wavelength of the transmitted signal in meters. The reflected heartbeat and respiration signals are amplified with a low noise amplifier (LNA) and then down-converted to the in-phase (I) and quadrature-phase (Q) receiver chains.

As shown in Fig. 1, the LO provides two identical frequency signals, one for the transmitter (TX) and the other for the receiver (RX). The LO signal for the receiver is further divided using a 90° power splitter to provide two orthonormal baseband outputs. Assuming that the amplitude noise is so small as to be ignored, an LO signal can be expressed as

$$T(t) = \cos(\omega t + \phi(t)) \tag{2}$$

where ω is the angular frequency, and $\phi(t)$ is the phase noise of the LO. The LO signal is amplified by a power amplifier (PA), feeds into the TX antenna, and is radiated into the air. Simultaneously, the RX antenna receives backscattered signals from the target. As shown in Fig. 1, the backscattered signals picked up by the RX antenna consist of two components: one is the backscattered signal from the heart and the other is from the stationary human body. The backscattered signal at the RX antenna, $R(t)$, is a time-delayed version of the transmitted signal and can be expressed as

$$\begin{aligned} R(t) \;=\; & A_R \cos\left[\omega t - \frac{4\pi d_0}{\lambda} - \frac{4\pi x(t)}{\lambda} + \phi\left(t - \frac{2d_0}{c}\right)\right] \\ & + A_C \cos\left[\omega t - \frac{4\pi d_0}{\lambda} + \phi\left(t - \frac{2d_0}{c}\right)\right] \end{aligned} \tag{3}$$

where A_R is the reflected signal magnitude from the heart, A_C is the reflected signal magnitude from the stationary human body, $2d_0/c$ and is the round-trip delay between the antenna and human. As the target distance is less than one meter, the channel can be assumed as a free space. Using the Friis electromagnetic wave propagation equation, A_R and A_C can be given by

$$A_R = \sqrt{\frac{2R_0 P_{TX} G_T G_R \lambda^2 \sigma_h L_h}{(4\pi)^3 d_0^4}} \tag{4}$$

$$A_C = \sqrt{\frac{2R_0 P_{TX} G_T G_R \lambda^2 \sigma_C L_C}{(4\pi)^3 d_0^4}} \tag{5}$$

respectively, where R_0 is the input resistance of the bio-radar's receiver, σ_h and σ_C are radar cross sections (RCSs), and L_h and L_C are reflection losses of the heart and human body, respectively.

As can be seen in Fig. 1, the receiver cannot totally isolate the transmitter due to the inherent antenna mutual coupling and mixer RF-LO coupling. Therefore, the leakage signals from the TX also enter the receiver. These TX leakage signals, $L(t)$, can be expressed as

$$\begin{aligned} L(t) \;=\; & \sqrt{2\eta_{ANT} R_0 P_{TX} G_{RX}}\cos[\omega(t-\Delta t_1)+\phi(t-\Delta t_1)] \\ & +\sqrt{2\eta_{Mix} R_0}\cos[\omega(t-\Delta t_2)+\phi(t-\Delta t_2)] \end{aligned} \tag{6}$$

where η_{ANT} is the TX leakage level between TX and RX antenna, η_{Mix} is the TX leakage level due to mixer RF-LO coupling, and Δt_1 and Δt_2 are the time delays between these TX leakage signals and the LO signal. Before further discussion, it is important to recognize that $\phi(t)$ in (2), (3), and (6) is related with the phase noise from the same LO except for time delays.

With a quadrature receiver, the received signal (3) and the LO signal (2) are mixed, and the output is band-pass filtered. In order to simplify the forthcoming analysis, the frequency response of the band-pass filter (BPF) is characterized approximately with an ideal rectangular transfer function, and its low-end frequency and high-end cutoff frequency are denoted as f_L and f_H, respectively. The resulting baseband signals will then be

$$\begin{aligned} B_I(t) \;=\; & A_R\sqrt{G_{RX}}\cos\left[\theta_h + \frac{4\pi x(t)}{\lambda} + \Delta\phi_h(t)\right] \\ & +A_C\sqrt{G_{RX}}\cos[\theta_C + \Delta\phi_c(t)] \\ & +\sqrt{2\eta_{ANT} R_0 P_{TX} G_{RX}}\cos[\theta_{L1} + \Delta\phi_{L2}(t)] \\ & +\sqrt{2\eta_{Mix} R_0}\cos[\theta_{L2} + \Delta\phi_{L2}(t)] + n_T(t) + n_{1/f}(t) \end{aligned} \tag{7}$$

$$\begin{aligned} B_Q(t) \;=\; & A_R\sqrt{G_{RX}}\sin\left[\theta_h + \frac{4\pi x(t)}{\lambda} + \Delta\phi_h(t)\right] \\ & + A_C\sqrt{G_{RX}}\sin[\theta_C + \Delta\phi_c(t)] \\ & + \sqrt{2\eta_{ANT}R_0P_{TX}G_{RX}}\sin[\theta_{L1} + \Delta\phi_{L2}(t)] \\ & + \sqrt{2\eta_{Mix}R_0}\sin[\theta_{L2} + \Delta\phi_{L2}(t)] + n_T(t) + n_{1/f}(t) \end{aligned} \quad (8)$$

respectively, where G_{RX} is the receiver gain, including the conversion gain of the mixer, $n_T(t)$ is the thermal noise, including receiver noise figure, $n_{1/f}(t)$ is the baseband $1/f$ noise from the mixer and baseband circuits, and $\Delta\phi_h(t)$, $\Delta\phi_C(t)$, $\Delta\phi_{L1}(t)$ and $\Delta\phi_{L2}(t)$ are the residual phase noises of reflected heart signal, clutter signal, antenna leakage signal, and mixer leakage signal, respectively. In addition, θ_{L1} and θ_{L2} are the constant phase shifts dependent on the time delay, Δt_1 and Δt_2. Also, θ_h and θ_C are the constant phase shifts dependent on the nominal distance to the target.

$$\theta_h \approx \theta_C = \frac{4\pi d_0}{\lambda} + \theta_0 \quad (9)$$

where, θ_0 is the phase shift at the reflection surface of the human body. The residual phase noises in (7) and (8) are given by

$$\Delta\phi_h(t) \;\approx\; \Delta\phi_C(t) = \phi(t) - \phi\left(t - \frac{2d_0}{c}\right) \quad (10)$$

$$\Delta\phi_{L1,2}(t) \;=\; \phi(t) - \phi(t - \Delta t_{1,2}) \quad (11)$$

respectively. Now, the received signals are digitized using an analog-to-digital converter (ADC). Finally, DSP block are used to separate superimposed heart and respiration signals, to combine quadrature channels, and to determine the heart rate. Generally, the heartbeat is calculated by various detection algorithms, such as zero crossing, autocorrelation, and Fourier transform [8].

3. SNR ANALYSIS

3.1. Theory

In a wireless bio-radar sensor, the backscattered signal from the heart should be stronger than other noise sources at the receiver's baseband output. This is very similar to a general radar system's SNR concept. In order to calculate the SNR value, we should know the magnitude of the signal and the noise power. The magnitude of the signal at the baseband depends on the received power and phase modulation.

Noise sources include residual phase noises from the LO, additive white Gaussian noise (AWGN), and the baseband $1/f$ noise of the mixer and of the baseband analog circuits.

First, the magnitude of the signal power at the baseband is given by radar theory. For example, the signal power at the baseband I channel, S_I, is equal to the mean squared received voltage divided by the input impedance and can be given by

$$\begin{aligned} S_I &= \frac{A_R^2 G_{RX} \overline{\cos\left(\theta_h + \frac{4\pi x(t)}{\lambda}\right)^2}}{R_0} \\ &= \frac{2P_{TX} G_T G_R G_{RX} \lambda^2 \sigma_h L_h \overline{\cos\left(\theta_h + \frac{4\pi x(t)}{\lambda}\right)^2}}{(4\pi)^3 d_0^4} \end{aligned} \tag{12}$$

Assuming perfect power combining and small angle approximation, the signal power is given by

$$S_I \approx \frac{P_{TX} G_T G_R G_{RX} \sigma_h L_h \overline{x^2(t)}}{2\pi d_0^4} \tag{13}$$

Next, we calculate the residual phase noise power. The residual phase noise includes the phase noise by the heart signal itself, the stationary human body reflection, the antenna leakage signal, and the mixer leakage signal. Because the frequency range concerned in a bio-radar sensor system is less than 10 Hz, the phase noise itself may be large enough to affect the signal detection. However, when the same oscillator is used for transmitting and down-converting operations, the phase noise of the received signal is correlated with that of the LO, and the phase noise is dramatically reduced. In radar applications, such as bio-radar, this phase noise reduction phenomenon is called the range correlation effect [4].

A quantitative characterization of the relation between range and phase noise can be done in the frequency domain. The power spectral density (PSD) of $\Delta\phi_h(t)$, $S_{\phi_h}(f_\Delta)$ at offset frequency, f_Δ is given by

$$S_{\Delta\phi_h}(f_\Delta) = S_\phi(f_\Delta)\left[4\sin^2\left(2\pi\frac{d_0 f_\Delta}{c}\right)\right] \tag{14}$$

where $S_\phi(f_\Delta)$ is the PSD of the LO itself. Equation (14) indicates that the range correlation effect gives a high pass filter effect on phase noise with respect to offset frequency. This effect is positive for detection in

a bio-radar system, because the heart and respiration signals are very low frequency signals.

Assuming that the typical values for d_0 and f_Δ are 50 cm and 10 Hz, respectively, the value of $d_0 f_\Delta / c$ will be on the order of 10^{-9}. Therefore, the small angle approximation is valid, and residual phase noise is simplified by

$$S_{\Delta\phi_h}(f_\Delta) \approx S_\phi(f_\Delta)\left[16\pi^2 \frac{{d_0}^2 {f_\Delta}^2}{c^2}\right] \tag{15}$$

Since the close-in phase noise has a -30 dB/decade slope, the phase noise can be defined by the phase noise at the 1 Hz, $S_\phi(1)$, as follows

$$S_{\phi_h}(f_\Delta) \approx \frac{S_\phi(1)}{(1\,\text{Hz})^{-3}} f_\Delta^{-3} \tag{16}$$

An equation of residual phase noise can be found by combining (15) and (16),

$$S_{\Delta\phi_h}(f_\Delta) \approx S_\phi(1)\left(\frac{f_\Delta}{1\,\text{Hz}}\right)^{-3}\left[16\pi^2 \frac{{d_0}^2 {f_\Delta}^2}{c^2}\right] \tag{17}$$

The mean square residual phase noise in the time domain is the integral of the spectrum over the received frequencies,

$$\begin{aligned}\overline{\Delta\phi_h(t)^2} &= \int_{f_L}^{f_H} S_{\Delta\phi_h}(f_\Delta) df_\Delta \\ &= 16\pi^2 (1\,\text{Hz})^3 S_\phi(1) \frac{d_0^2}{c^2} \ln\left[\frac{f_H}{f_L}\right]\end{aligned} \tag{18}$$

Now, the residual phase noise power from received signal is given by

$$\begin{aligned}N_{\Delta\phi_h} &= \frac{A_R^2 G_{RX} \overline{\cos(\Delta\phi_h(t))^2}}{R_0} \\ &\approx \frac{2P_{TX} G_T G_R G_{RX} \lambda^2 \sigma_h L_h \overline{\Delta\phi_h(t)^2}}{(4\pi)^3 d_0^4}\end{aligned} \tag{19}$$

An equation of residual phase noise from the received signal can be found by combining (18) and (19),

$$N_{\Delta\phi_h} = \frac{P_{TX} G_T G_R G_{RX} \sigma_h L_h}{2\pi f^2 d_0^2} S_\phi(1) \ln\left(\frac{f_H}{f_L}\right) \tag{20}$$

Similarly, the residual phase noise by clutter, antenna leakage, and mixer leakage are as follows,

$$N_{\Delta\phi_C} = \frac{P_{TX}G_TG_RG_{RX}\sigma_C L_C}{2\pi f^2 d_0^2} S_\phi(1) \ln\left(\frac{f_H}{f_L}\right) \tag{21}$$

$$N_{\Delta\phi_{L1}} = 32\pi^2 \eta_{ANT} P_{TX} G_{RX} S_\phi(1) \ln\left(\frac{f_H}{f_L}\right)\left(\frac{\Delta t_1}{2}\right)^2 \tag{22}$$

$$N_{\Delta\phi_{L2}} = 32\pi^2 \eta_{Mix} S_\phi(1) \ln\left(\frac{f_H}{f_L}\right)\left(\frac{\Delta t_2}{2}\right)^2 \tag{23}$$

Finally, there are two other intrinsic noise sources: AWGN and $1/f$ noise. The AWGN power is expressed by,

$$N_T = 8G_{RX} \cdot kTB \cdot NF \tag{24}$$

where k is Boltzman's constant, T is the absolute temperature, and B is the bandwidth. The bandwidth is very small in a bio-radar sensor system, and the AWGN power is also very small. For example, the heart rate is normally between 0.83 and 1.5 Hz (50 and 90 beats per minute) [7]. Assuming the system bandwidth of 10 Hz, the AWGN power is about -164 dBm. In addition, $1/f$ noise is caused by mixer output. Choosing a passive mixer that minimizes $1/f$ noise will minimize the amount of baseband noise. Now, the $1/f$ noise power can be defined by the measured mixer noise at the 1 Hz, $P_{1/f}(1)$, as follows

$$N_{1/f} = \int_{f_L}^{f_H} P_{1/f}(1) f^{-1} df = P_{1/f}(1) \ln\left(\frac{f_H}{f_L}\right) \tag{25}$$

Now, all the noises are combined at the mixer output after they have been converted to their values in the baseband. Because six noise sources are uncorrelated, the noise powers are simply added. Therefore, the SNR value for the bio-radar sensor is given by

$$\text{SNR} = \frac{S_I}{N_{1/f} + N_T + N_{\Delta\phi_h} + N_{\Delta\phi_C} + N_{\Delta\phi_{L1}} + N_{\Delta\phi_{L2}}} \tag{26}$$

3.2. SNR results

In the previous sections, SNR equations have been derived. In order to show the usefulness of the derived equations, this section presents numerical results of SNR for various cases. The parameters used in the SNR calculation are summarized in Table 1.

Table 1. Parameters of a wireless bio-radar sensor system.

System Specification	Parameter
Operating Frequency	2.4 GHz ISM band
Filter Low-cutoff Frequency (f_L)	0.5 Hz
Filter High-cutoff Frequency (f_H)	10 Hz
Receiver Gain (G_{RX})	10 dB
Antenna Gain ($G_T = G_R$)	0 dBi
Output Power (P_{TX})	0 dBm
Heart Parameters (σ_h)	6.8e-3
Body Clutter Parameters (σ_C)	0.5
Heart Reflectivity (L_h)	-60 dB
Human Body Reflectivity (L_C)	-3 dB
Maximum Heart motion ($x(t)$)	1.22 cm
Receiver Noise Figure	6.0 dB
LO Phase Noise at 1Hz ($S_{\phi(t)}(1)$)	58 dB/Hz
Antenna Leakage (η_{ANT})	-20 dB
Mixer RF-LO Isolation (η_{Mix})	-50 dB

The parameters of a wireless bio-radar sensor are divided into two groups: one group is due to the human body and the other due to transceiver design. The transceiver parameters are chosen considering the state-of-the-art, low-cost circuit performance, including a free-running oscillator without external PLL circuits. The human body parameters are chosen considering the general human body characteristics. Normally, the size of a human heart is about 12 cm in length, 9 cm in breath, and 6 cm in thickness [9]. Therefore, we assumed the heart as a sphere with a diameter of 12 cm and calculated the heart RCS (σ_h) using a normal RCS equation for a sphere [10]. Based on the dielectric properties of body tissues in [11] and [12], the path loss of a 2.4 GHz CW signal in a human body can be calculated. For a 2.4 GHz CW signal, the path loss is about -15 dB in a human body. Only about 4% of the signal is reflected from the heart, and total heart reflectivity (L_h) becomes -60 dB. Fig. 2 shows the overall path loss of a 2.4 GHz CW signal in a human body. Also, the stationary part of the human body and the surrounding environment are considered

when estimating the RCS of the clutter. This RCS value is more straightforward to calculate since it is not restricted to an area of motion. A clutter RCS estimate of $0.5\,\mathrm{m}^2$ will be used in these calculations. The expected amplitude of motion of the mitral valve along the long axis of the heart, $x(t)$, was expected to be 1.49 cm at age 20 and 1.22 cm at age 84 [7]. We selected the minimum value, assuming a home monitoring service in an elderly user.

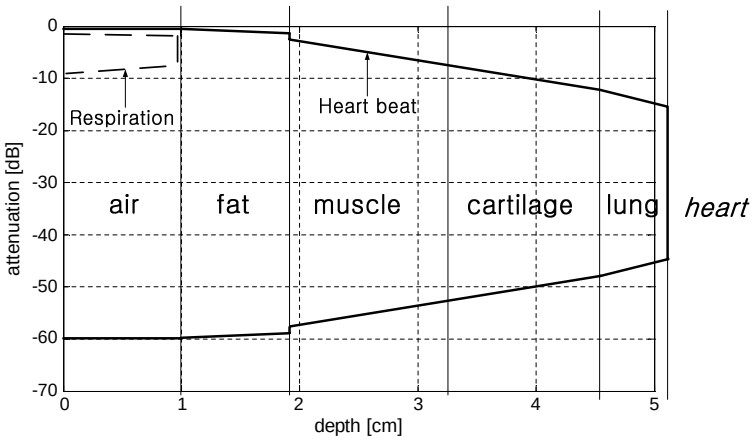

Figure 2. Path loss of 2.4 GHz signal in a human body.

In the calculation of the SNR of the wireless bio-radar sensor, it is important to know the phase noise at 1 Hz offset frequency, $S_{\phi(t)}(1)$. However, it is very difficult to measure the closed-in phase noise of the free-running oscillator using a general spectrum analyzer. Then, we considered the phase noise measurement setup shown in Fig. 3. An HMC38LP4 free-running oscillator from Hittite was used for the measurement. The oscillator generates a CW signal at a frequency of 2.45 GHz with 3 dBm output power. The CW signal with phase noise is divided into two paths. One path was time delayed using a delay line cable and connected to a Skyworks SKY73009 mixer. The other path was connected to the LO port of the mixer. The baseband output of the mixer was measured with an HP89441A signal analyzer. To eliminate the DC offset, the phase shifter was tuned until the DC component of the baseband signal, as viewed on an oscilloscope, was zero. The loss through the cables and phase shifter was compensated with an HP1975A amplifier. The baseband noise spectrum from 1 Hz to 1 KHz was measured with a 1-Hz resolution bandwidth and root-mean square (rms) averaged over ten measurements. The baseband noise spectrum measurements were converted to a phase noise equivalent by

calculating the ratio of the measured noise power.

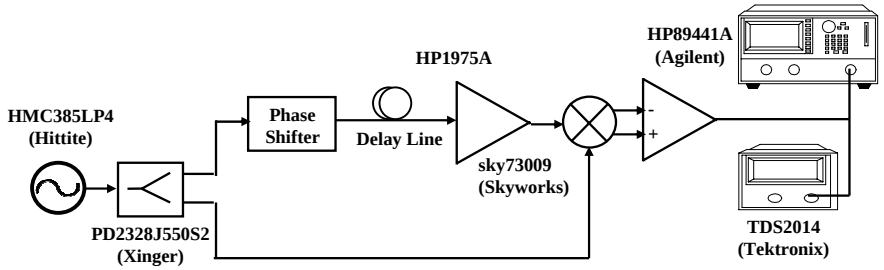

Figure 3. Experiment setup for the residual phase noise measurement.

The measured voltage output at the VSA can be found as follows.

$$\begin{aligned} V_{measured} &= KA_{LO}\cos(\omega t + \phi(t)) \times A_{RF}\sin(\omega t + \phi(t - \tau_{delay})) \\ &= \frac{1}{2}KA_{LO}A_{RF}[\sin(2\omega t + \phi(t) + \phi(t - \tau_{delay})) \\ &\quad + \sin(\phi(t) - \phi(t - \tau_{delay}))] \end{aligned} \tag{27}$$

where K is the down-conversion coefficient of the receiver composed of the mixer and the base-band amplifier. As the RF signal multiplied by LO signal passes the low-pass baseband amplifier, the measured baseband signal can be approximated as

$$V_{measured} = K'\sin(\phi(t) - \phi(t - \tau_{delay})) \cong K'[\phi(t) - \phi(t - \tau_{dalay})] \tag{28}$$

where $K' = KA_{LO}A_{RF}$ is the overall conversion coefficient. The K' coefficient represents the phase-to-voltage conversion ratio of the range-correlation effect, which means the noise cancellation between the original signal and the time-delayed signal. The overall phase-to-voltage coefficient in Equation (28) should be measured before the calculation of the phase noise equivalent from the measured baseband voltage. We have measured 72 points for the phase difference between the RF and LO ports. The phase-to-voltage curve fitting from the measured samples is shown in Fig. 4.

The measured residual phase noise is shown in Fig. 5. The measured value is below $-110\,\mathrm{dB/Hz}$ at 1 Hz offset frequency. The baseband noise is converted to an RF phase noise equivalent by using the phase-voltage curve of Fig. 4 and the equation of range correlation effect (14). Now, using the measured value of the residual phase noise at 1 Hz, we can calculate the noise powers due to the phase noise.

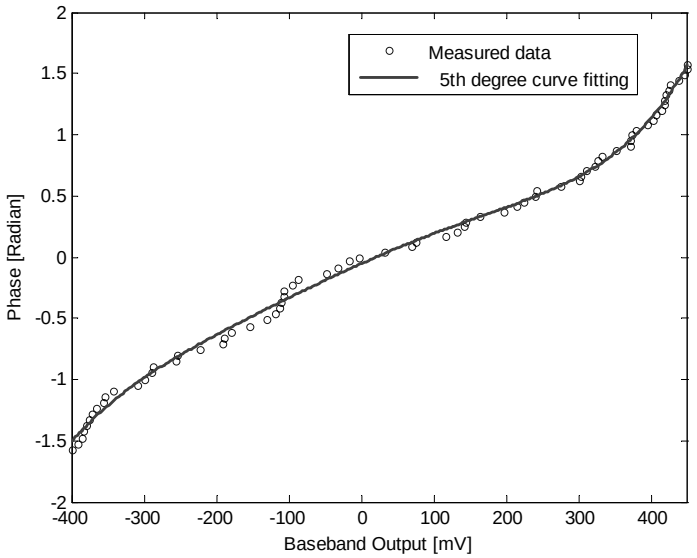

Figure 4. Graph for phase-voltage conversion coefficients in residual phase noise measurement.

Based on the above analysis and measurement results, we calculate the SNR value of a wireless bio-radar sensor [13]. Fig. 6(a) shows the result of SNR with respect to target distance in case of -20 dB TX leakage. Noise powers lower than the thermal noise power have been omitted. As the target distance from the antenna increases, the received signal power decreases due to the space loss between the target and the antenna. Hence, the SNR decreases. When the target is about 50 cm away from the antenna, the noise power is as strong as the received signal. Consequently, the heart signal will not be detected beyond this distance. One noise source is not dominant for all ranges: the clutter phase noise will be dominant close to the target, and the residual phase noise due to TX leakage will be dominant further from the target. In order to increase the sensitivity of the bio-radar system, it is imperative to reduce the dominant noise source, that is, the residual phase noise due to antenna mutual coupling. Fig. 6(b) shows the identical analysis results, except for the value of TX leakage. As the antenna isolation is enhanced by 20 dB, the SNR value increases to about 7 dB at the 50 cm detection range. From the numerical results, it can be concluded that the TX leakage should be reduced in order to increase the detection range of the wireless bio-radar sensor.

4. WIRELESS BIO-RADAR SENSOR DESIGN AND MEASUREMENT RESULTS

4.1. Wireless Bio-radar Sensor Design

Based on the SNR analysis previously discussed, the wireless bio-radar sensor was designed and fabricated. The bio-radar sensor was implemented in a 4-layer printed circuit board. We consider a portable, low-cost bio-radar sensor with a 50 cm detection range. With the previous analysis, the path loss was calculated at 120 dB for a target range of 50 cm, and the signal bandwidth was about 10 Hz. The output power of the designed wireless bio-radar sensor was set to 0 dBm for a low-cost design without an additional power amplifier.

Figure 7 shows a photograph of a 2.4 GHz wireless bio-radar sensor for heartbeat and respiration detection. The LO and TX signals are generated by an HMC385LP4 MMIC VCO. The frequency of the VCO is 2.4 GHz ISM band. The power divider divides the power equally to the TX antenna and LO port of the quadrature mixer. As discussed in the previous section, with the same LO sources for transmitting and receiving, the range correlation effect will greatly decrease the phase noise at the baseband to a level that can be ignored. The 2.4 GHz

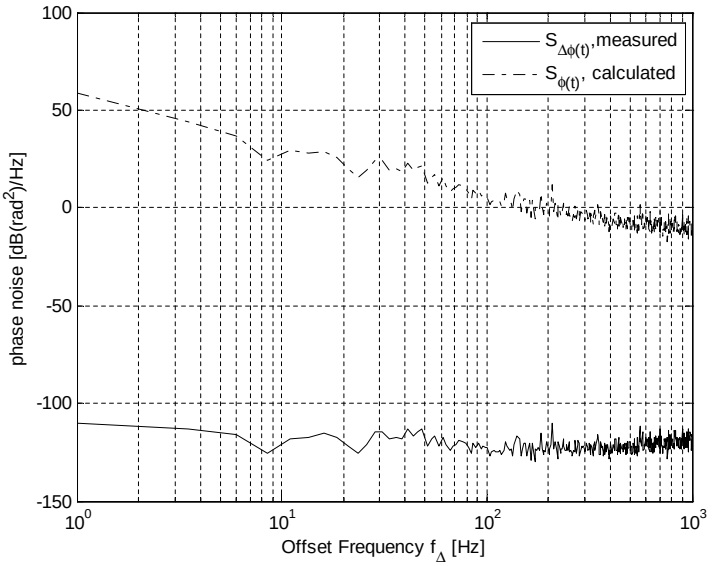

Figure 5. Measured baseband residual phase noise and calculated phase noise of a free-running oscillator (Hittite HMC38LP4).

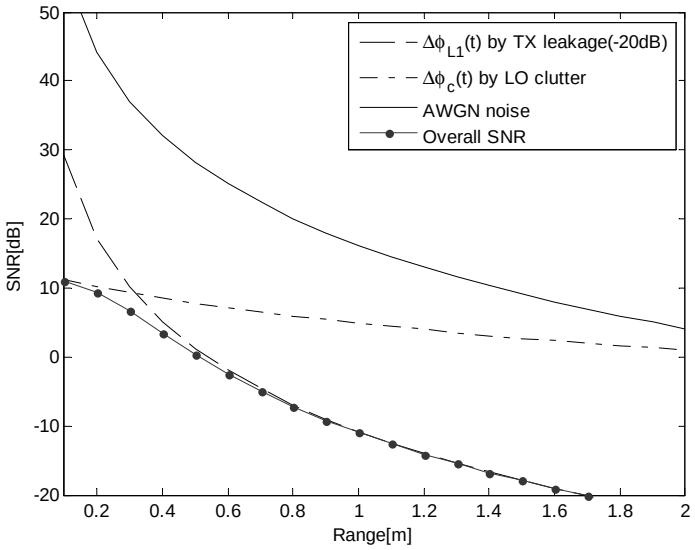

(a)

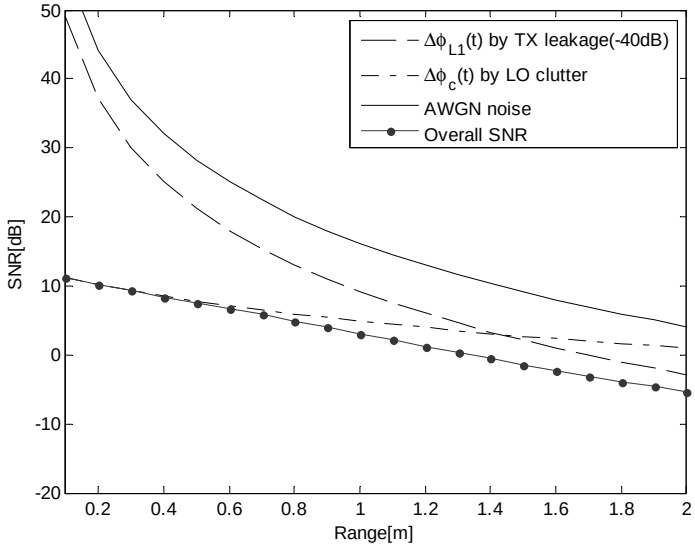

(b)

Figure 6. SNR value of wireless bio-radar sensor with respect to target distance: (a) in case of -20 dB TX leakage, (b) in case of -40 dB TX leakage.

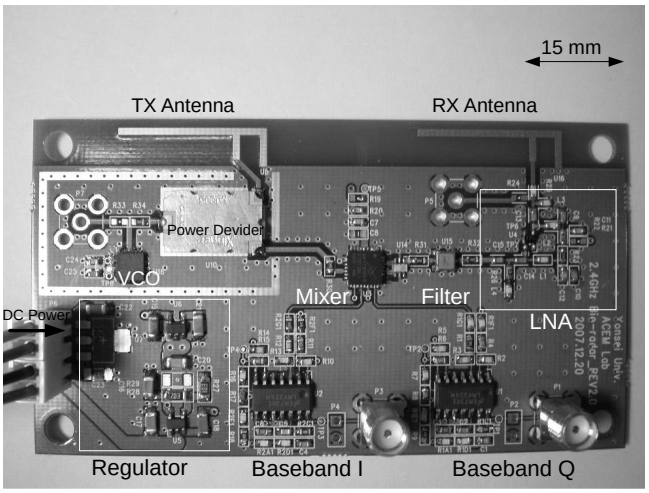

Figure 7. Photograph of a wireless 2.4 GHz bio-radar sensor for heartbeat and respiration detection.

band-pass filter eliminates the spurious interference signal from the RX antenna. The SKY73009 quadrature mixer provides a quadrature output. Down-converted signal from the mixer output goes into the baseband circuits.

Heartbeat and respiration signals acquired from the bio-radar sensor are mixed up, so there is a need to separate them. The baseband module is designed to separate the heartbeat and respiration signals acquired from the I/Q channels of the bio-radar sensor and increase the SNR of the signals. The baseband module consists of an offset circuit, a band pass filter circuit, and an amplifier to separate the heartbeat and respiration. The band pass filter for respiration has a frequency bandwidth of 0.05 to 0.5 Hz. The band pass filter for heartbeat has a frequency bandwidth of 1 to 30 Hz.

TX and RX dual antennas are used to increase the antenna isolation and then reduce TX leakage. As the measured value of an antenna mutual coupling is about -20 dB, the detection range is to be about 50 cm from our analysis. The PCB size, including dual antennas, is 90 mm $\times$ 50 mm. The VCO part is isolated using a shield metal to reduce unpredicted interference power on receiver circuits. The regulator provides $+5$ V and $+/-3$ V. Detailed component descriptions are given in Table 2.

Table 2. Actual device components used for implementing a 2.4 GHz wireless bio-radar sensor.

Components	Description (Company)
Antenna	Inverted F Antenna Printed on a board
VCO	HMC385LP4 (Hittite)
Power divider	PD2328J5050S2
LNA	Design using 2SC5508 transistor (NEC)
Filter	SA2441AM saw filter (SAWNICS)
Balun	LDB212G4005C (Murata)
Mixer	sky73009 demodulator (SKYWORKS)
+3 V regulator	LP2992 (National Semiconductor)
−3 V regulator	LT1964 (Linear technology)
Baseband OP Amp	LMV321 (National Semiconductor)

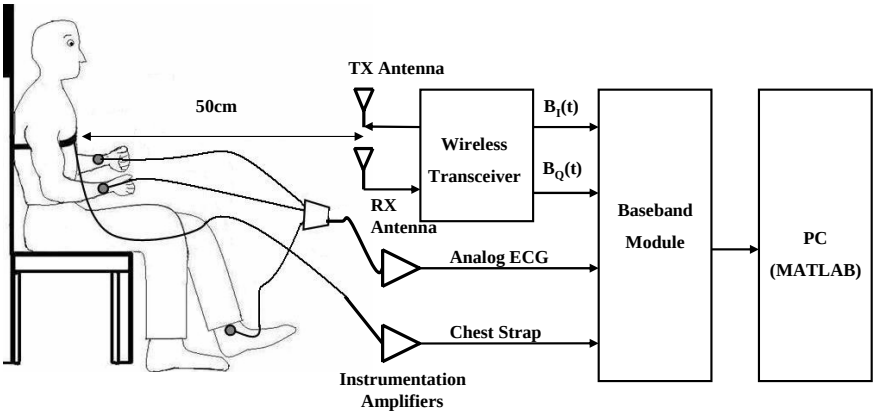

Figure 8. Measurement setup for heartbeat and respiration detection.

4.2. Measurement Results

In order to verify the performance of the developed bio-radar sensor, a reference ECG signal and reference respiration signal were measured simultaneously, as shown in Fig. 8. The band-pass filter for the reference 3-lead ECG and reference respiration have frequency bandwidths of 0.5 to 40 Hz and 0.05 to 5 Hz, respectively. Two reference signals, and two heartbeat and respiration signals for each

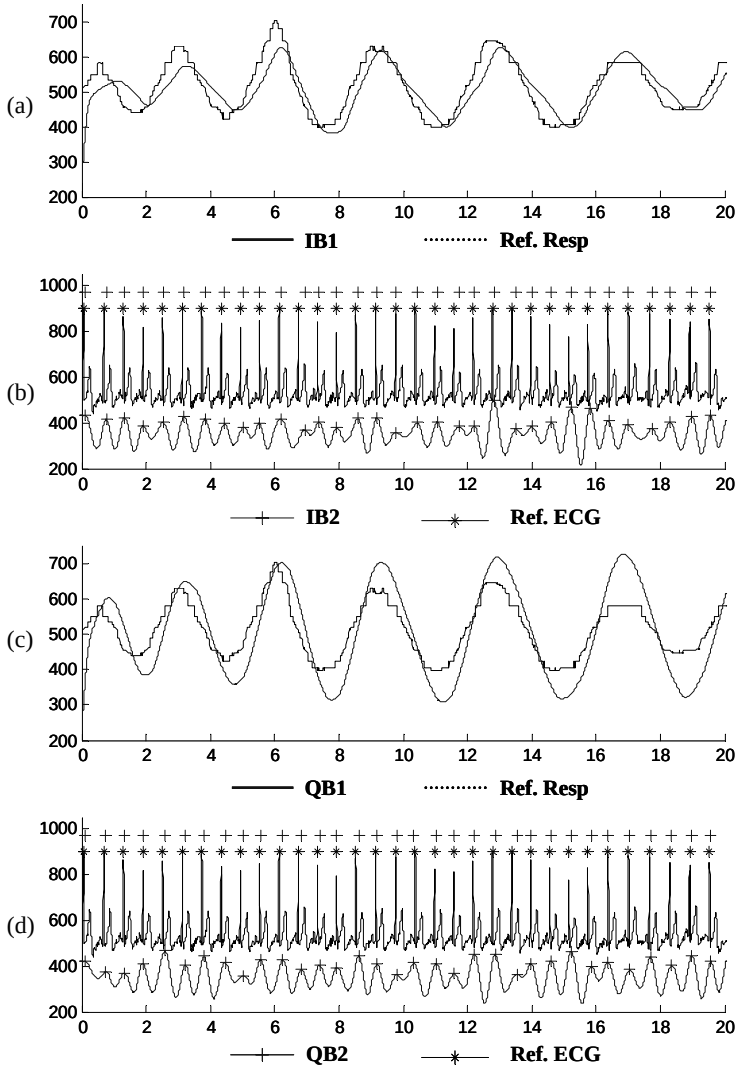

Figure 9. Measurement results of bio-radar signals at the distance of 50 cm (a) respiration signal of I channel; (b) heartbeat of I channel; (c) respiration signal of Q channel; (d) heartbeat of Q channel.

channel of the bio-radar system, making six ports in total, were sampled at a frequency of 480 Hz with 10-bit-resolution A/D using a PIC18F452 (Microchip, USA). The digitized signals were transmitted to a laptop for display.

Figure 9 shows the results processed during 20 seconds for bio-radar signals acquired from the wireless bio radar sensor system at the distance of 50 cm. The bio-radar sensor signal was processed by the 300th FIR low pass filter with a cutoff frequency of 0.5 Hz. After separating heartbeat and respiration, these signals were compared with the reference signal. The bio-radar signal was measured on the frontal side of the subject. Figs. 9(a) and (c) show respiration signals extracted from the I and Q channels, respectively. The extracted respiration signals have close relations to the reference respiration signals. Both the respiration rates are the same, but there exists a phase difference between them. The heartbeat signals extracted from I and Q channel are shown in Figs. 9(b) and (d), respectively. The upper signal and lower signal in each panel show the reference ECG and heartbeat respectively. The heartbeat signals almost coincide with the reference ECG signals, but they are somewhat different in terms of peak to peak interval.

5. CONCLUSION

When system engineers are developing a wireless bio-radar sensor, the SNR is a key design parameter. Accordingly, in this study, a wireless bio-radar sensor was designed using SNR concepts. To calculate the SNR value, the path loss and noise power are necessary. Then, the path loss is derived using the electromagnetic characteristics of human tissues and all kinds of noise sources are calculated. Especially, we measured a residual phase noise of a typical free-running oscillator and used its value for the SNR analysis. Based on these analysis and measurement results, a compact, low-cost 2.4 GHz direct conversion wireless bio-radar sensor was designed and implemented in a 4-layer printed circuit board. The developed sensor consists of two printed antennas, a voltage-controlled oscillator, an I/Q demodulator and analog circuits. With an output power of 0 dBm and a free-running oscillator without PLL circuits, a exact heartbeat and respiration signals were measured when using a distance of 50 cm. Measurement results show that the heart rate and respiration accuracy was found to be very high. We verified that the wireless bio-radar sensor could detect heartbeat and respiration well without contact and our SNR analysis could be effective tool to design a wireless bio-radar sensor.

REFERENCES

1. Lubecke, V. M., O. Boric-Lubecke, A. Host-Madsen, and A. E. Fathy, "Through-the-Wall radar life detection and

monitoring," *IEEE MTT-S Int. Microwave Symposium Digest*, 769–772, May 2007.

2. Lin, J. C., "Non-invasive microwave measurement of respiration," *Proceedings of the IEEE*, Vol. 63, No. 10, 1530, 1975.
3. Droitcour, A. D., O. Boric-Lubecke, V. M. Lubecke, and J. Lin, "A microwave radio for Doppler radar sensing of vital signs," *IEEE MTT-S Int. Microwave Symposium Digest*, 175–178, 2001.
4. Droitcour, A. D., O. Boric-Lubecke, V. M. Lubecke, J. Lin, and G. T. A. Kovac, "Range correlation and I/Q performance benefits in single-chip silicon doppler radars for non-contact cardiopulmonary monitoring," *IEEE Transactions on Microwave Theory Technique*, Vol. 52, 838–848, March 2004.
5. Park, B.-K., O. Boric-Lubecke, and V. M. Lubecke, "Arctanget demodulation with dc offset compensation in quadrature Doppler radar receiver systems," *IEEE Transactions on Microwave Theory Technique*, Vol. 55, 1073–1079, May 2007.
6. Nguyen, D., S. Yamada, B.-K. Park, V. M. Lubecke, O. Boris-Lubecke, and A. H. Madsen, "Noise considerations for remote detection of life signs with microwave Doppler radar," *Proceedings of the 29th Annual International Conference of the IEEE EMBS*, 1667–1670, August 2007.
7. Droitcour, A., "Non-contact measurement of heart and respiration rates with a single-chip microwave doppler radar," Ph.D. Thesis, Stanford University, June 2006.
8. Lohman, B., O. Boric-Lubecke, V. M. Lubecke, P. W. Ong, and M. M. Sondhi, "A digital signal processor for Doppler radar sensing of vital signs," *Proceedings of IEEE 23rd Annual Engineering in Medicine and Biology Society Conference*, Vol. 4, 3359–3362, 2001.
9. Henry, G., *Anatomy of the Human Body*, Philadelphia, Lee & Febiger, 1918.
10. Chang, K., *RF and Microwave Wireless Systems*, Wiley Science, 2000.
11. Staderini, E. M., "UWB radar in medicine," *IEEE AESS Systems Magazine*, Vol. 17, 13–18, January 2002.
12. Gabriel, C., "Compilation of the dielectric properties of body tissues at RF and microwave frequencies," http://niremf.ifac.cnr.it/.
13. Fan, Z., S. Qiao, H.-F. Jiang Tao, and L.-X. Ran, "Signal descriptions and formulations for long range UHF RFID readers," *Progress In Electromagnetics Research*, PIER 71, 109–127, 2007.